

Interaction of Finite NaCl Crystals with Infrared Radiation*

T. P. MARTIN†

Department of Physics and Materials Research Laboratory, University of Illinois, Urbana, Illinois 61801

(Received 24 November 1969)

Low-temperature measurements of the infrared absorption of small crystals of NaCl are made in the acoustical-mode frequency region. A large contribution to the absorption coefficient of small crystals is found which is not temperature-dependent and is not due to impurities. This absorption is observed to be more sensitive to the density of the powdered sample than to the crystal size. The fundamental absorption of small crystals of NaCl is also measured. The frequency of the peak absorption is seen to be insensitive to the number of crystals per unit volume. The material at the crystal interface strongly affects the shape of the transmission curve. A Green's-function calculation of the surface-induced infrared absorption is made. The surface is simulated by setting nearest-neighbor force constants between atoms in adjacent (001) planes equal to zero.

I. INTRODUCTION

IN the harmonic approximation, an alkali halide crystal with translational symmetry absorbs light only at the frequency of the long-wavelength transverse optical mode of vibration ω_{TO} . If the translational symmetry is destroyed by making one or more dimensions of the crystal finite, the low-frequency acoustical modes acquire a dipole moment and absorb light also. Furthermore, the fundamental absorption does not occur at ω_{TO} . The latter effect was first pointed out by Fröhlich¹ when he showed that the fundamental absorption of a small alkali halide sphere will occur at a frequency between ω_{TO} and the long-wavelength longitudinal optical mode ω_{LO} . If the sphere is small compared to the wavelength of the incident light, a mode with uniform polarization will absorb the light. The frequency of this mode is given by

$$\omega_s^2 = [(\epsilon_0 + 2\epsilon) / (\epsilon_\infty + 2\epsilon)] \omega_{TO}^2. \quad (1)$$

The static and high-frequency dielectric constants of the small crystal are denoted by ϵ_0 and ϵ_∞ . The dielectric constant of the medium in which the crystals are embedded is ϵ . The extension of Fröhlich's formula to include this last parameter was made by Axe and Pettit.² Fuchs and Kliewer³ and Englman and Ruppin⁴ have shown that the mode with uniform polarization is not the only optically active mode in a small sphere. A series of surface modes with frequencies between ω_{TO} and ω_{LO} should absorb light. With the inclusion of retardation, their calculations show that polariton states exist not only between ω_{TO} and ω_{LO} but also below ω_{TO} and that light will be absorbed because of anharmonic polariton-polariton scattering in these states. There have been several brief descriptions of experiments by

Hass⁵ and others^{2,6-8} that tend to support some of these theoretical predictions. However, there seems to be a need for more experimental work. One set of experiments described in this paper shows the effect of temperature, surrounding media, and neighboring crystals on the infrared absorption of small crystals of NaCl.

Infrared absorption by the acoustical modes of small crystals has been predicted by Rosenstock.⁹ The model he used for a calculation neglected long-range Coulomb forces and assumed the modes of vibration had either a sinusoidal or an exponential spatial dependence. Recently, an exact calculation of the normal modes of a semi-infinite ionic crystal has been made by Tong and Maradudin.¹⁰ However, because of the exact nature of the calculation, their model of the crystal contains only a small number of atomic layers. In this paper, we have made a Green's-function calculation assuming neither sinusoidal solutions nor very thin crystals. We have assumed, however, that the surface can be simulated by setting nearest-neighbor force constants between atoms in adjacent planes equal to zero.

Apparently, there has been only one attempt made to observe surface-induced infrared absorption by acoustical modes. Hadni *et al.*¹¹ have observed an increased far-infrared absorption in samples of alkali halide crystals which have been ground up. The size, shape, and perfection of the resulting crystallites were not reported. In this paper, we report measurements at liquid-helium temperature of the infrared absorption in the acoustical-mode region of small rectangular NaCl crystals 0.5 and 10.0 μ in size.

The theoretical and experimental techniques used to study the fundamental infrared absorption are different from those used to study the weak low-frequency

* Research supported in part by the Advanced Research Projects Agency under Contract No. SD-131.

† Present address: Department of Physics, Lehigh University, Bethlehem, Pa.

¹ H. Fröhlich, in *Theory of Dielectrics* (Oxford University Press, Oxford, 1948), 2nd ed., pp. 153-155.

² J. D. Axe and G. D. Pettit, Phys. Rev. **151**, 676 (1966).

³ R. Fuchs and K. L. Kliewer, J. Opt. Soc. Am. **53**, 319 (1968).

⁴ R. Englman and R. Ruppin, J. Phys. C1, 614 (1968).

⁵ M. Hass, Phys. Rev. Letters **13**, 429 (1964).

⁶ W. W. Pultz and W. Hertl, Spectrochim. Acta **22**, 573 (1966).

⁷ R. Summitt, Spectrochim. Acta **23A**, 2857 (1967).

⁸ T. P. Martin, Phys. Rev. **177**, 1349 (1969).

⁹ H. B. Rosenstock, J. Chem. Phys. **23**, 2415 (1955).

¹⁰ S. Y. Tong and A. A. Maradudin, Phys. Rev. **181**, 1318 (1969).

¹¹ A. Hadni, G. Morlot, X. Gerbaux, D. Chanal, F. Brehat, and P. Strimer, Compt. Rend. **260**, 4973 (1965).

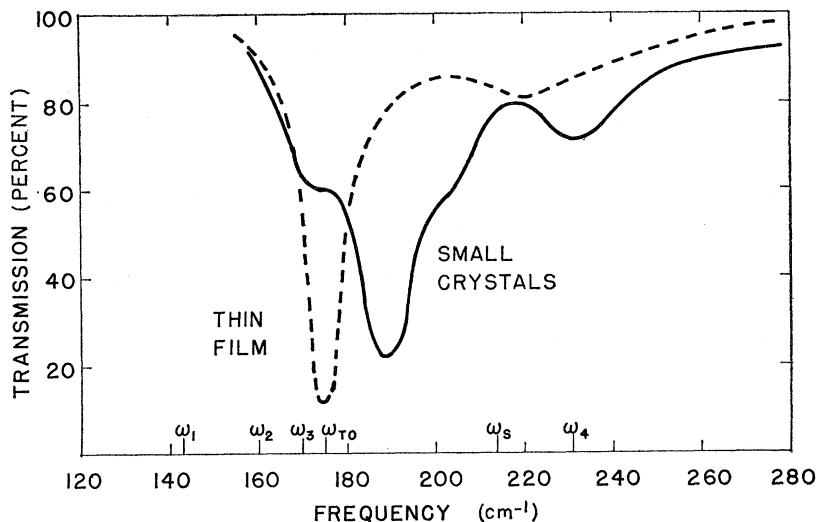


FIG. 1. Comparison of the infrared transmission through a thin film and through small crystals of NaCl at 7°K.

acoustical-mode absorption. It is convenient, therefore, to discuss the two frequency regions separately.

II. MEASUREMENT OF FUNDAMENTAL INFRARED ABSORPTION

Because of the long-range forces between ions, the fundamental infrared absorption of an alkali halide crystal is dependent on its size and shape. Calculations of the absorption have been made using convenient models, e.g., well-separated spheres in air.^{3,4} However, it is difficult to obtain these conditions experimentally. In this section, we describe experiments which indicate what parameters are important enough to be included in a more realistic model.

A. Procedure

Small crystals were prepared in the following way. A saturated water solution of NaCl was sprayed into the air. After waiting 15 sec for the largest drops to fall, the remaining mist was allowed to settle onto a substrate made of polyethylene. The droplets were allowed to evaporate leaving small NaCl crystals firmly adhering to the substrate. This process was repeated until the desired number of crystals per unit area was obtained. When observed from above through a microscope, the individual crystals in the powder were found to be square. However, the dimension of the side of the crystal perpendicular to the substrate was smaller than that of the other sides by a factor as small as $\frac{1}{3}$. The transmission of a substrate with crystals on it and a substrate without crystals was measured using a Beckman IR11 spectrometer. For the low-temperature measurements, both substrates were mounted in a liquid-helium cryostat.

B. Results and Discussion

In order to be able to recognize size effects in small crystal samples, we first examined the infrared trans-

mission of a thin-film sample. Figure 1 shows the transmission at 7°K of a thin film of NaCl relative to the transmission of its sapphire substrate. The film is 1 μ thick. Since a thin film should have maximum infrared absorption at ω_{TO} ,¹² we will use the frequency of minimum transmission 175 cm^{-1} as a definition of ω_{TO} . There is a secondary transmission minimum at 220 cm^{-1} which is attributed to two-phonon absorption.

If an experimental sample of small crystals is to correspond to the theoretical model, the crystals must be well separated compared to the wavelength of light. Therefore, less than 4% of a surface should be covered with 10- μ crystals. We covered 1–2% of the area of a 4-mil polyethylene sheet with crystals. Since one layer with such small coverage would absorb very little light, 50 sheets were fused together by heating. The crystals in such a sample were well separated and completely surrounded by polyethylene. During the process of fusion, the crystals did not change their orientation or position.

Figure 1 shows the transmission at 7°K of this sample relative to the transmission of polyethylene prepared in the same way but with no NaCl. The maximum absorption by the small crystals can be seen to occur at a frequency higher than ω_{TO} . However, there is a secondary transmission minimum at ω_{TO} as well as at 205 cm^{-1} and 232 cm^{-1} . The shift of the maximum absorption to frequencies higher than ω_{TO} is in qualitative agreement with the theoretical predictions of the absorption by small spheres.^{3,4} Several relevant calculated frequencies have been indicated in Fig. 1 to show that the agreement is not quantitative. The frequency labeled ω_s was obtained from Eq. (1) using for ϵ , ϵ_0 , and ϵ_∞ the values 2.3, 5.62, and 2.25. The frequencies labeled ω_1 , ω_2 , ω_3 , and ω_4 are the positions of absorption peaks calculated by Ruppin and Englman.⁴ In this calculation, the crystals were assumed to be 10- μ NaCl

¹² R. Fuchs and K. L. Kliewer, Phys. Rev. 140, A2076 (1965).

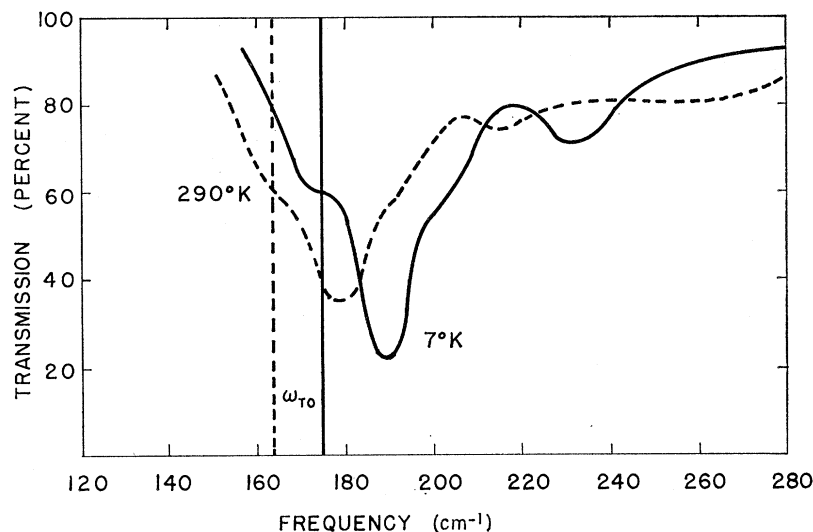


FIG. 2. Comparison of the infrared transmission through small crystals of NaCl at 7 and 290°K.

spheres well separated in air. The frequency ω_4 does coincide with a measured secondary transmission minimum. The coincidence is probably fortuitous because this minimum may correspond to the two-phonon absorption observed at 220 cm^{-1} in a thin-film sample. Two-phonon absorption for a thin-film sample and for a small crystal sample would not occur at the same frequency if one of the two phonons corresponded to the shifted fundamental mode of vibration. We conclude that the absorption of well-separated small cubes of NaCl in polyethylene differs in several ways from the calculated absorption of small spheres in air. The peak surface-mode absorption of the cubes occurs at a frequency much closer to ω_{TO} . The cubes show a secondary absorption peak only at ω_{TO} . No absorption peaks occur at the calculated frequencies below ω_{TL} or at ω_1 , ω_2 , and ω_3 .

The transmission of the small crystal sample described above was also measured at 290°K (Fig. 2). Clearly, the principal effect of raising the temperature is to shift the entire curve to lower frequencies. In order to emphasize this point, both the low- and the high-temperature values of ω_{TO} have been indicated. Since no new features are brought out by making the measurements at 7°K, the remaining transmission curves in this section were measured at room temperature.

The effect on the absorption of increasing the density of crystals on a surface was also studied. A relatively dense sample was prepared by covering about 30% of the two surfaces of a polyethylene sheet with small crystals. Each of the two surfaces was then covered with another sheet of polyethylene and the sandwich fused together. A comparison of the infrared transmission of this high-density sample and the low-density

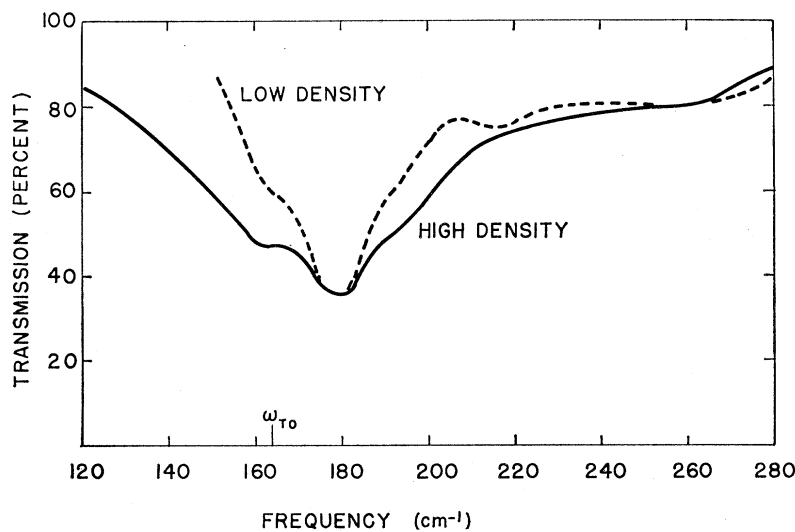


FIG. 3. Comparison of the infrared transmission through samples made with large and with small numbers of NaCl crystals per unit area.

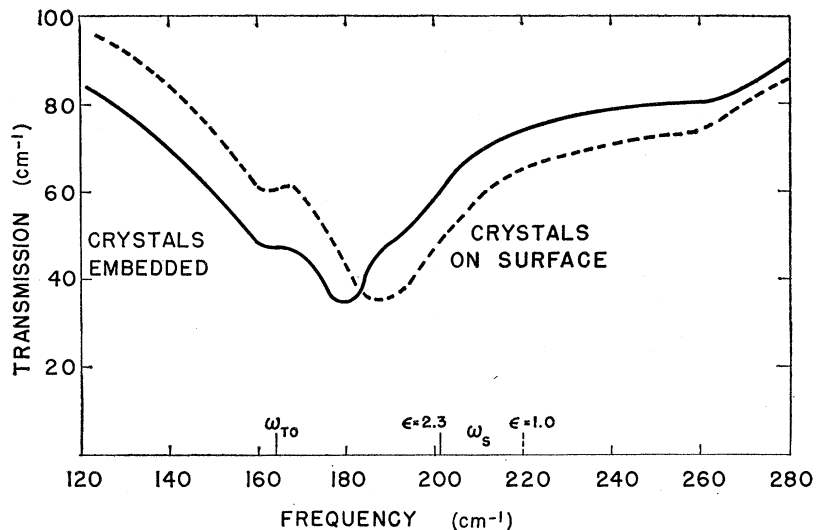


FIG. 4. Comparison of the infrared transmission through NaCl crystals on the surface of polyethylene and through crystals completely surrounded by polyethylene.

sample described earlier is shown in Fig. 3. There appears to have been no shift in either the main transmission minimum or the secondary minimum at ω_{TO} because of interaction among the crystals. The high-density sample does have a broader absorption band. In particular, there is considerably more absorption at frequencies smaller than ω_{TO} . Each crystal will have a different dielectric environment determined by the arrangement of its neighboring crystals. However, this may not be the explanation for the observed broadening.

In the experiments above, we were careful to make the environment of the crystals fairly uniform. Each crystal was completely surrounded by polyethylene. The transmission of small crystals situated at an air-polyethylene interface is shown in Fig. 4. Here five crystal surfaces are in air and the sixth in polyethylene. Also shown in Fig. 4 is the transmission of crystals completely embedded in polyethylene. For both samples there is a secondary transmission minimum at ω_{TO} . However, the peak absorption of the embedded crystals occurs at a lower frequency. The direction of this frequency shift is in agreement with Eq. (1). Two values of ω_s are indicated in the figure (corresponding to ϵ equal to 1.0 and 2.3). We conclude that the frequency of peak surface-mode absorption is strongly affected by the material at the crystal surfaces. It is therefore necessary that realistic boundary conditions be used when making calculations for comparison with experiment.

III. CALCULATION OF SURFACE-INDUCED INFRARED ABSORPTION

The motion of atoms in a crystal can be represented by 3η coupled equations, where η is the number of atoms in the crystal. If the crystal has translational symmetry, the number of coupled equations can be

reduced to the number of degrees of freedom in a unit cell. If the crystal is imperfect, Lifshitz has shown that the problem can still be greatly simplified.¹³ Using a Green's-function technique, the number of coupled equations is not equal to 3η but equal to the number of coordinates needed to define the defect. Thus, for a localized point defect the equations of motion of the crystal are easily written. If the defect is planar, for example a surface, the Green's-function technique gives as few as $3n$ coupled equations, where n is the number of atoms in the plane. This still seems to be a formidable problem, but the translational symmetry in two dimensions allows an even simpler formulation.

A. Formulation and Results

The notation and some of the equations described in Ref. 14 will be used in this section. We will begin by writing a general expression for defect-induced infrared absorption in an ionic crystal in terms of the T matrix of the imperfect crystal.

$$K(\omega) = \frac{4\pi(n_\infty^2 + 2)^2}{9vcn(\omega)} \omega \left(\frac{E_\kappa^2 \eta \pi}{2\mu\omega_{TO}} \delta(\omega - \omega_{TO}) \right. \\ \left. + \frac{N}{(\omega^2 - \omega_{TO}^2)^2} \lim_{\epsilon \rightarrow 0} \text{Im} \sum_{l\kappa} \sum_{l'\kappa'}' E_\kappa M_\kappa^{-1} \right. \\ \left. \times T'_{\alpha\alpha}(l\kappa, l'\kappa', \omega^2 - i\epsilon) E_{\kappa'} M_{\kappa'}^{-1} \right), \quad (2)$$

where v is the volume of the crystal, and n_∞ and $n(\omega)$ are the real parts of the index of refraction at high frequency and at arbitrary frequency. Each atom in a unit cell l is labeled with an index κ . The effective

¹³ I. M. Lifshitz, Nuovo Cimento Suppl. 3, 716 (1956).

¹⁴ T. P. Martin, Phys. Rev. 170, 779 (1968).

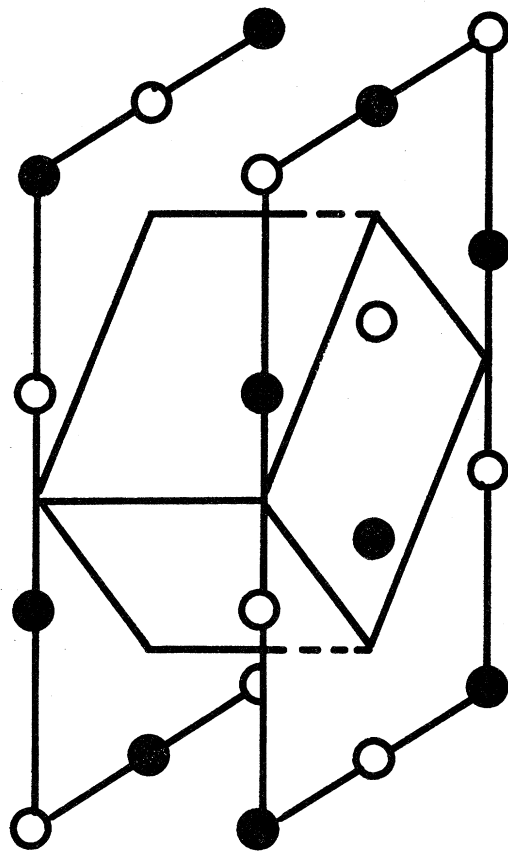


FIG. 5. A unit cell in a portion of the defect space for a surface defect in NaCl. The surface is generated by setting nearest-neighbor force constants between atoms in these adjacent planes equal to zero.

charge of the atom in the perfect crystal at site κ is E_κ . The number of unit cells in the crystal has been denoted by η , the number of defects by N , and the reduced mass by μ . The incident light is assumed to be polarized in the α direction. The prime indicates that the summation over the atoms should be limited to the space of one defect. The projection of the T matrix onto the space of the defect is denoted by T' . The defect space includes only those atoms which interact differently in the perfect crystal and imperfect crystal. We will assume in this calculation that only the atoms at the surface interact differently. Specifically, the surface will be simulated by decreasing to zero the nearest-neighbor force constant between atoms in adjacent (001) planes. A portion of the defect space for this model is shown in Fig. 5. Since the defect space contains an infinite number of atoms, the problem must be further reduced. This can be done using the translational symmetry in the x , y directions. In order to use the translational symmetry, it is useful to define a new unit cell containing four atoms (Fig. 5). This is a unit cell for both the defect space and the perfect crystal. The Green's functions of the perfect crystal

are normally defined and calculated in terms of the more usual unit cell containing two atoms. This unit cell allows the NaCl crystal to be described by an fcc lattice and a Brillouin zone as shown by the dotted lines in Fig. 6. If the four-atom unit cell is used, both the lattice and the Brillouin zone are rectangular solids (Fig. 6). Note that six segments of the 14-sided Brillouin zone extend beyond the six-sided Brillouin zone. New branches in the phonon dispersion curves for the four-atom unit cell are formed when these segments are fitted back into the six-sided Brillouin zone. Such a procedure gives the relation between the wave vector and branch indices of normal modes using the two-unit cells.

Because of the translational symmetry of the surface, we can assume plane-wave solutions in the x and y directions. We will see that this reduces the size of the T matrix of interest from $3n \times 3n$ to 12×12 . The transformation to be applied is

$$S(l_x, l_y, k_x, k_y) = (N_x N_y)^{-1/2} \times \exp\{i[k_x U_x^0(l_x, \kappa) + k_y U_y^0(l_y, \kappa)]\},$$

where $(N_x N_y)$ is the number of unit cells in the xy plane. If this transformation is applied to the summation in Eq. (2), the summation can be written

$$\sum_{l_z \kappa} \sum_{l_z' \kappa'} \left(\sum_{l_x l_y} \frac{E_\kappa}{M_\kappa^{1/2}} S(l_x' l_y', k_x k_y) \right) \times S^{-1} T S(l_z \kappa, l_z' \kappa', k_x' k_y', k_x k_y, \omega^2 - i\epsilon) \times \left(\sum_{l_x' l_y'} \frac{E_{\kappa'}}{M_{\kappa'}^{1/2}} S^{-1} (l_x' l_y', k_x' k_y') \right).$$

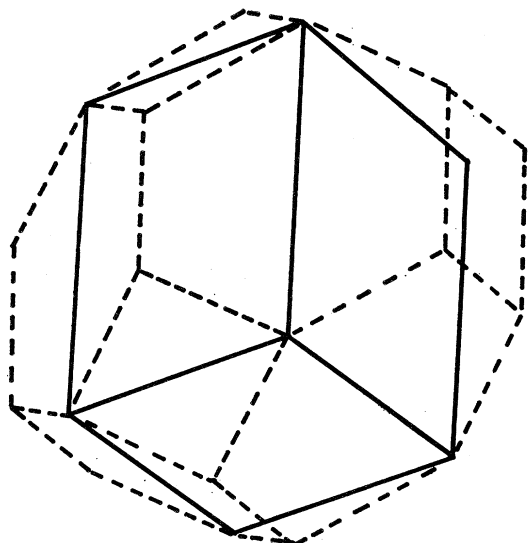


FIG. 6. The first Brillouin zone of an NaCl crystal based on the four-atom unit cell (solid line) and on the two-atom unit cell (dotted line).

The expressions in large parentheses are the effective charge of a layer of atoms for a mode with quantum numbers $k_x k_y$ or $k_x' k_y'$. Evidently, this effective charge is zero unless k_x, k_y and k_x', k_y' are zero. Using this result in Eq. (2), the difference in the absorption coefficient of the perfect and imperfect crystal can be written

$$\Delta K(\omega) = \frac{4\pi N_x N_y N (n_\infty^2 + 2)^2}{cvn(\omega) 9} \frac{\omega}{(\omega^2 - \omega_{TO}^2)^2} \times \sum'_{l_z \kappa, l_z' \kappa'} \frac{E_\kappa E_{\kappa'}}{(M_\kappa M_{\kappa'})^{1/2}} \lim_{\epsilon \rightarrow 0} \text{Im} \bar{T}_{\alpha\alpha}(l_z \kappa, l_z' \kappa', \omega^2 - i\epsilon), \quad (3)$$

where we have defined a planar \bar{T} matrix as

$$\bar{T}_{\alpha\alpha}(l_z \kappa, l_z' \kappa', \omega^2 - i\epsilon) = (S^{-1}TS)_{\alpha\alpha}(l_z \kappa, l_z' \kappa', 00, 00, \omega^2 - i\epsilon). \quad (4)$$

The evaluation of the T matrix for a crystal with point imperfections has been described many times. Although we are dealing with a planar imperfection, a detailed exposition of the calculation is not needed. However, a brief descriptive outline will be given emphasizing the extended nature of the defect.

T , and therefore \bar{T} , has nonzero elements for only those values of l_z defining atoms within the surface. The dimensions of \bar{T} are, therefore, 12×12 . This matrix can be factored using the point symmetry of the two-dimensional space group of the planar defect. The space group of our surface model is $P4mm$. The corresponding point group is $4mm$ or C_{4v} . Because we have defined the surface by changing only the force constant between nearest-neighbor atoms across the surface, the \bar{T}_{xx} and \bar{T}_{yy} elements will be zero. That is, light normally incident on the surface will give no surface contribution to its absorption coefficient. We will calculate the absorption of light incident parallel to the surface and polarized in the z direction. This calculation involves the nonzero \bar{T}_{zz} elements. The \bar{T}_{zz} elements form a 4×4 factor of \bar{T} after the reduction by point symmetry. This is the dimensionality of the final form of the problem. The planar T matrix can be expressed in terms of a planar Green's-function matrix for the perfect crystal \bar{G} and a planar-defect matrix defining the imperfection $\bar{\Delta}$:

$$\bar{T} = \bar{\Delta} (1 - \bar{G} \bar{\Delta})^{-1}.$$

The relation between the planar matrices and the more usual matrices is indicated by Eq. (4). The evaluation of the real and imaginary parts of the elements of the Green's-function matrix of a perfect crystal requires a knowledge of the vibrational eigenvalues and eigenvectors of the perfect crystal. It is easy to show that the evaluation of the planar Green's functions involves only those solutions of the perfect crystal for which $k_x = k_y = 0$. The eigenvalues of interest are shown in Fig. 7. Here, we have used the results of a shell-model

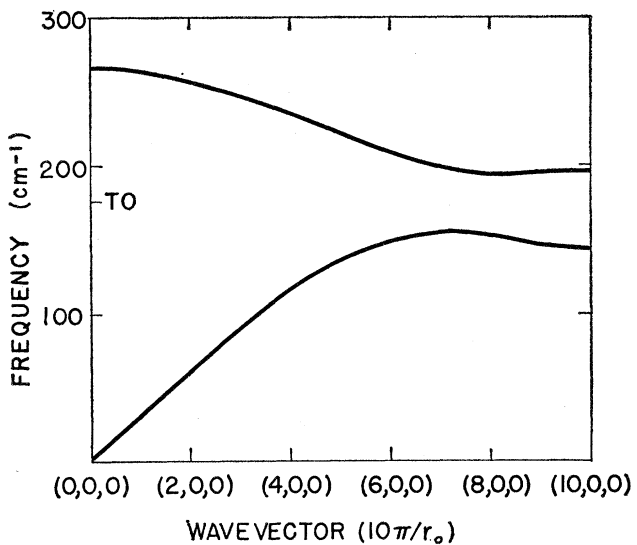


FIG. 7. Longitudinal phonon-dispersion curves of NaCl.

calculation by Macdonald *et al.*¹⁵ Singularities in the density of states of these one-dimensional phonon-dispersion curves will occur at frequencies with zero slope. These singularities will be infinities, and they should also occur in the Green's functions and the absorption coefficient. Such infinities are a peculiarity of the planar-defect problem. Another characteristic of the absorption spectrum is a sudden drop to zero at the maximum frequency of the branch. The infinities and sharp cutoff indicate that the surface-induced infrared absorption might offer an important probe of characteristic frequencies of the phonon-dispersion curves of the perfect crystal along a given direction in k space.

The dashed line in Fig. 8 describes the density of states as a function of frequency in the acoustical-mode region. The two singularities for this calculated curve do not show up as infinities but merely as rounded peaks. This is due to the approximate nature of the computer calculation. The solid line in Fig. 8 shows the surface-induced absorption in NaCl for light incident parallel to the surface and polarized perpendicularly to the surface. The only parameter used to describe the surface is the change in the nearest-neighbor force constant between atoms in adjacent (001) planes. This parameter was taken to be $-15\,000$ erg/cm². We see that the absorption coefficient roughly reflects the density of states. There are no additional peaks that would suggest a resonance phonomenon. In fact, even the singularity peaks in the density of states do not affect the absorption sufficiently to show up in the computer calculation. The only characteristic frequency of the perfect crystal well defined by the absorption curve is the high-frequency cutoff.

¹⁵ H. F. Macdonald, Miles V. Klein, and T. P. Martin, Phys. Rev. **177**, 1292 (1969).

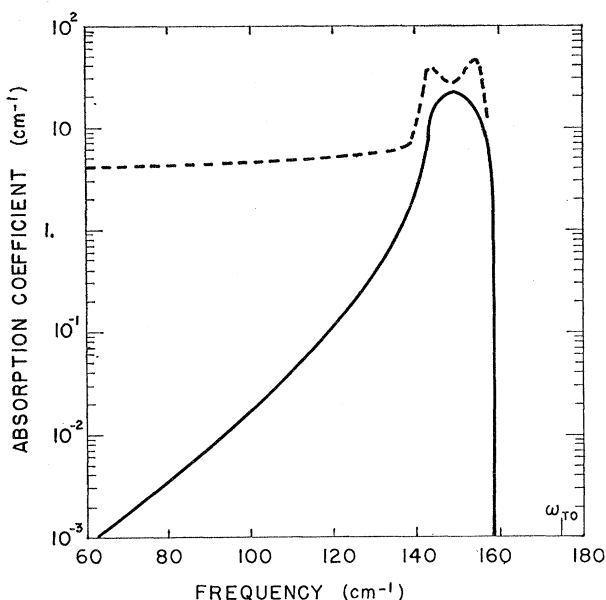


FIG. 8. Calculated surface-induced infrared absorption in NaCl (solid line) and the one-dimensional density of states corresponding to the dispersion curves in Fig. 7 (dotted line).

B. Discussion

In this calculation, we have used a very simple model of the surface since we are interested in only the qualitative features of surface-induced infrared absorption by NaCl. The model is unrealistic in several ways. Although the two planes of atoms on either side of the surface are uncoupled, the long-range coupling across the surface remains that of a perfect crystal. In addition, the imperfect crystal does not obey the condition of rotational invariance. In spite of these deficiencies in the model, we think several conclusions applicable to experiment can be made. The effects of the infinities in the one-dimensional density of states will not be easily observed in absorption measurements. Even the computer calculation shows a smooth absorption curve. The integrated surface-induced absorption is comparable to integrated impurity-induced absorption if the number of surface atoms is the same as the number of impurity atoms. The absorption cutoff will define the maximum phonon frequency on a given branch along a given direction in k space. The polarization of the light will determine the branch, and the crystallographic orientation of the surface will determine the direction in k space.

Preparing a sample to measure these characteristic frequencies would be very difficult. The light must go through on the order of 1000 surfaces before there will be appreciable absorption. In general, any imperfection which destroys the xy translational symmetry of the surfaces will broaden the absorption edge. Therefore, the surfaces must be parallel, flat, and many wavelengths in extent.

IV. MEASUREMENT OF LONG-WAVELENGTH INFRARED ABSORPTION

A. Procedure

The above calculation shows that the infrared absorption by the acoustical modes of an ionic crystal slab has several interesting features. However, the sample would be very difficult to prepare. Therefore, we have measured the absorption of small rectangular solids of NaCl. The absorption spectrum of such small crystals is not expected to resemble that of slabs except perhaps in integrated intensity. The calculations indicated that if the ratio of surface atoms to volume atoms is 0.001 or larger, surface-induced absorption would be observable. This ratio corresponds to a powder composed of cubes smaller than $2\ \mu$ on a side.

We prepared small crystals of NaCl in the following manner. Sodium chloride powder was evaporated in a partial vacuum of 2×10^{-2} mm Hg. The evaporated NaCl collected as a white powder on the sides of the bell jar. The bell jar was opened to the atmosphere and the NaCl scraped off. An examination of this NaCl powder under an electron microscope showed the individual crystals to be approximately $0.5\ \mu$ on a side. Powder with individual crystals as large as $10\ \mu$ was also prepared. The method used to grow these larger crystals was described in Sec. I. The NaCl powder was pressed into wafers of various thicknesses. The pressure used varied from 1000 to 12 000 psi.

Since the surface absorption was expected to be weak, absorption due to other processes had to be reduced. It was necessary that the sample be pure to one part in 10^5 or 10^4 in order to eliminate impurity-induced infrared absorption. The concentration of both metal and nonmetal impurities was measured using emission and mass spectroscopy. The total impurity concentration

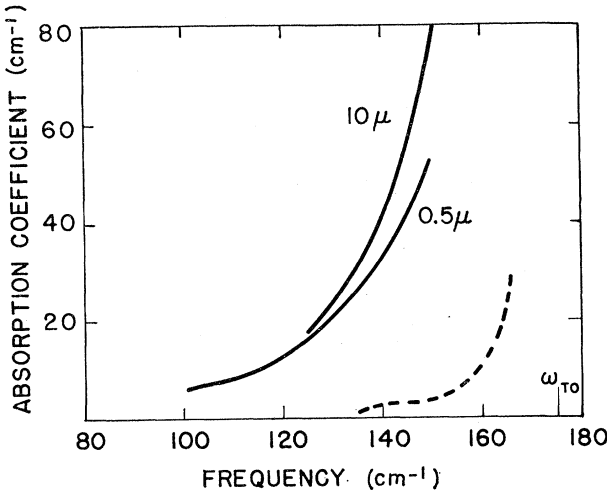


FIG. 9. Long-wavelength infrared absorption at 7°K by NaCl crystals of indicated size. Absorption by a large single crystal (dotted line).

was found to be less than one part in 10^4 . Two-phonon absorption was reduced by making the absorption measurement at low temperatures.

The wafers of NaCl powder were mounted in a liquid-helium cryostat. The transmission was measured using a Beckman IR11 spectrometer. In order to obtain the absorption coefficient from the transmission measurement, it was necessary to account for the multiple reflections from the surfaces of the wafer. This was done using the following expression, which relates the absorption coefficient K to the transmittance T of the sample, reflectance R of one surface, and thickness d of the sample:

$$T = (1 - R)^2 e^{-Kd} / (1 - R^2 e^{-2Kd}). \quad (5)$$

In the case of weak absorption, R can be expressed in terms of the real part of the index of refraction n :

$$R = (n - 1)^2 / (n + 1)^2.$$

The index of refraction is given approximately by

$$n^2 = \epsilon_\infty + (\epsilon_0 - \epsilon_\infty) / (1 - \omega^2 / \omega_{TO}^2).$$

The static and high-frequency dielectric constants are denoted by ϵ_0 and ϵ_∞ , the reststrahl frequency by ω_{TO} .

In using Eq. (5), we have assumed that scattering losses are negligible. Certainly there is no appreciable scattering from individual crystals since the wavelength of the incident light is 5 to 100 times larger than the largest dimension of the crystals. Scattering from clusters of crystals would be important only at very low sample densities.

B. Results and Discussion

Figure 9 shows the measured absorption coefficient of the powder samples pressed into thin wafers. The average size of the crystals in the two samples is 0.5 and 10.0 μ , as indicated in the figure. Both samples show considerably more absorption than a single crystal. In Sec. III, surface-induced infrared absorption by acoustical modes was shown to be proportional to the surface-to-volume ratio of the sample. However, the absorption is about the same in both of our samples. The large-crystal sample may even show slightly more absorption. Moreover, if the absorption were by acoustical modes, we would expect more structure in the spectrum. It would appear, therefore, that this low-frequency absorption is not by acoustical modes. What is its origin? The absorption appears to be due to a broadening of the strong reststrahl absorption at ω_{TO} . This immediately suggests an anharmonic effect enhanced by the small size of the crystal. Such an effect was checked by making the absorption measurement at higher temperatures. There was an increase in the absorption when the sample was measured at 80°K. However, this increase could be completely accounted for by the expected increase in absorption of a perfect

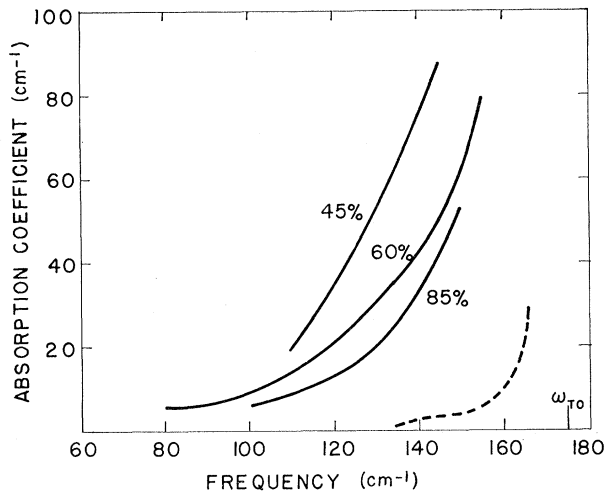


FIG. 10. Long-wavelength infrared absorption at 7°K by NaCl powder having the indicated percentage mass density of single-crystal NaCl. Absorption by a large single crystal (dotted line).

large crystal. So apparently we are not observing an anharmonic phenomenon.

The absorption mechanism may be indicated by the measurements shown in Fig. 10. Here, we see that the absorption depends strongly on the density of the wafer. That is, the absorption of a crystallite seems to be influenced by the proximity of its neighbors. Therefore, long-range forces must be an important consideration. In fact, polariton calculations for a sphere do indicate increased absorption at frequencies below ω_{TO} . Although a polariton calculation does partially take into account long-range forces, the technique to date is limited to samples with $10^{-40}\%$ of the density of NaCl, i.e., well-separated particles.

The series of curves in Fig. 10 suggests that there may be a residual absorption in the limit of 100% of the density of NaCl. If this limit could be approached experimentally, calculations similar to those of Sec. II would be more applicable. For such a sample, the surface could be well described by changing only short-range interactions in an infinite crystal. Unfortunately, the pressures necessary to attain such densities would probably introduce additional imperfections that would cloud the issue.

V. CONCLUSIONS

The fundamental infrared absorption of small ionic crystals is strongly affected by the dielectric properties of the materials at their boundaries. It will be necessary to use realistic boundary conditions at each surface in any calculation to be compared with experiment. The frequency of peak absorption was found to be the same for small crystals well-separated compared to the wavelength of the incident light and for crystals much closer

together. Therefore, it may not be necessary to include the effects of multiple scattering when making a calculation.

In principle, the surface-induced infrared absorption by acoustical modes will have infinities at frequencies where the appropriate one-dimensional dispersion curves have zero slope. A computer calculation using a simple surface model showed no peaks at these critical points, nor were there any peaks that might suggest a resonance phenomenon in the acoustical-mode region.

Small rectangular solids of NaCl showed strong absorption at acoustical-mode frequencies. The surface-

induced absorption had no structure, was insensitive to the particle size, and was independent of temperature. Therefore, we have not observed either surface-induced absorption by acoustical modes or an anharmonic broadening of the fundamental absorption. The effect is probably due to polariton scattering.

ACKNOWLEDGMENTS

The author is grateful to Dr. V. G. Mossotti for a chemical analysis of the samples and to Professor Miles V. Klein for several stimulating conversations.

Raman Spectra of GeO_2

J. F. SCOTT

Bell Telephone Laboratories, Holmdel, New Jersey 07733

(Received 25 November 1969)

Raman spectra of small single crystals of both the trigonal and tetragonal forms of germanium dioxide have been obtained. Frequencies and symmetries of the Raman-active optical phonons are given, and comparison is made with isomorphous α quartz and rutile. The temperature dependences of the spectra have been examined over the range 6–1100°K. The static dielectric constant and infrared reflectivity of the trigonal form have been calculated from the Raman data.

INTRODUCTION

GERMANIUM dioxide occurs in three stable forms at ambient temperatures.¹ The first form has the cassiterite (or rutile) tetragonal D_{4h}^{14} structure ($P4/mmm$) with octahedral coordination.² The second form has the trigonal D_3^{14} (32) structure of α quartz,³ with tetrahedral coordination. The third form is glassy, having the same short-range order of GeO_4 tetrahedra as the trigonal form, but lacking any long-range correlation.⁴ The tetragonal and trigonal crystalline forms differ substantially in their chemical properties, especially solubility, in their densities and indices of refraction. The glassy form resembles the trigonal in all these respects.

While a substantial amount of study of the optical properties of glassy GeO_2 has been made in the past,⁵ very little has been known about the crystalline varie-

ties, since single crystals do not occur naturally. The recent growth of small single crystals of both trigonal and tetragonal forms of GeO_2 has made the present Raman investigation possible. The motivation for the present study is several fold. Both crystalline varieties of GeO_2 have interesting device possibilities. The rutile form is hard, colorless, and transparent; it is highly inert and of consequent interest as an encapsulating material⁶ for germanium semiconductors. The quartz form is interesting from a device standpoint for all the reasons quartz is interesting: It is a hard, transparent, colorless piezoelectric with an index of refraction greater than that of quartz and a large enough birefringence (four times that of quartz) to make phase-matched nonlinear optical experiments possible. Both forms of GeO_2 have theoretical interest also: the rutile lattice has been the subject of several dynamical calculations recently⁷; quartz exhibits a well-studied phase transition⁸ and a unique hybrid-phonon excitation,⁹ as well as two modes (one infrared-active) with enough gain to produce stimulated Raman scattering,¹⁰ and it is of special interest to see which of the preceding attributes are also

¹ J. H. Muller and H. R. Blank, *J. Am. Chem. Soc.* **46**, 2338 (1924).

² X-ray studies first reported by A. W. Laubengauer and D. S. Morton, *J. Am. Chem. Soc.* **54**, 2303 (1932).

³ W. H. Zachariasen, *Z. Krist.* **67**, 226 (1928).

⁴ See, for example, T. G. Kujumzelis, *Z. Phys.* **100**, 221 (1935).

⁵ V. V. Obukhov-Denisov, N. N. Sobolev, and V. P. Cherenishev, *Izv. Akad. Nauk SSSR* **22**, 1083 (1958) [English transl.: *Bull. Acad. Sci. USSR* **22**, 1073 (1958)]; P. Flubacher, A. J. Leadbetter, J. A. Morrison, and B. P. Stoicheff, *J. Phys. Chem. Solids* **12**, 53 (1959). References to earlier work are given in the latter. V. P. Cherenishev, *Proc. (Trudy) Lebedev Inst.* **25**, 127 (1965). The most complete optical study of GeO_2 is given here. See also E. R. Lippincott, *J. Res. Natl. Bur. Std.* **61**, 61 (1958), for a conflicting IR spectrum.

⁶ See, for example, J. F. O'Hanlon, *Appl. Phys. Letters* **14**, 127 (1969).

⁷ See, for example, F. Matossi, *J. Chem. Phys.* **19**, 1543 (1951).

⁸ References to recent work are given in S. M. Shapiro, D. C. O'Shea, and H. Z. Cummins, *Phys. Rev. Letters* **19**, 361 (1967) and in Ref. 9.

⁹ J. F. Scott, *Phys. Rev. Letters* **21**, 907 (1968).

¹⁰ P. E. Tannerwald and D. L. Weinberg, *J. Quant. Electron.* **3**, 334 (1967); J. F. Scott, *ibid.* **3**, 693 (1967).